Design and Simulation of an Underactuated Finger Rehabilitation Exoskeleton based on Bionic Kinematics

Minghao Deng

School of Mechanical and Vehicle Engineering, Chongqing Jiaotong University, Chongqing, China

632413020313@mails.cqjtu.edu.cn

Abstract. Nowadays, stroke is the leading cause of death and disability in China, and the disability rate exceeds 80%. Approximately 80% of patients have upper limb functional disorders, and the impairment of fine hand movements is particularly significant. The effect of traditional rehabilitation treatment is limited, and the existing finger exoskeletons have problems such as insufficient bionics and poor adaptability to daily scenarios, which restrict the clinical rehabilitation effect. In response to the problem that finger rehabilitation exoskeletons can achieve a high degree of bionics and be close to daily life, based on the bionic principle of the four-bar linkage mechanism, a design scheme for an under-actuated finger rehabilitation exoskeleton with a serial topological transmission of connecting rods is proposed. The device uses an aviation aluminum alloy frame. The stiffness of the key load-bearing parts reaches 18 GPa, and the weight is less than 200 g. Compared with traditional stainless steel materials, the mass is reduced by 42%. Simulate the coordinated relationship between adjacent phalanges during the flexion and extension movements of human fingers, achieve multi-joint linkage driven by a single power source, and it is suitable for the rehabilitation of hand motor function in stroke patients. Based on the patients' grasping needs in various life scenarios, kinematic simulations and analyses of grasping small balls made of rubber, oak, and stainless steel were carried out. The feasibility of the design of an underactuated finger rehabilitation exoskeleton based on bionic kinematics was verified.

Keywords: Exercise Enhancement, Exoskeleton, Underactuation, Mechanism Design, Simulation Analysis.

1. Introduction

According to a survey by the World Health Organization, there are more than one billion people with disabilities of varying degrees in the world, and this number is still increasing [1]. Among them, the proportion of people with finger disabilities is quite high. In daily life, finger motor function disorders have a significant impact on patients' ability to grasp objects and perform work operations, resulting in a serious decline in their quality of life [2]. In traditional medical methods, doctors will provide professional treatment to patients. However, the cost is relatively high, and the training intensity and efficiency are not very high [3].

Currently, exoskeleton-based hand function rehabilitation trainers mainly include rigid exoskeletons and flexible exoskeletons. Most rigid exoskeletons are relatively heavy, and their driving parts are also quite large. They are not easy to carry and cannot meet the needs of patients for self - self-rehabilitation at home. However, their advantage is that they can provide sufficient power, and the control position is relatively accurate. There are mainly linkage-type hand exoskeletons and desktop hand exoskeleton trainers, etc [4-6]. Therefore, in order to help or guide patients to return to normal life, it is necessary to design a rehabilitation exoskeleton for underactuated upper-limb fingers.

The index finger rehabilitation exoskeleton developed by North China University of Science and Technology is based on the NOKOV optical motion capture experiment. It innovatively designs a crank-slider-flexible diagonal rod composite mechanism and realizes a dual-motion mode through a flexible hinge: when the end resistance is greater than 8.79 N, the self-locking protection mechanism is triggered. A fabric transmission belt is used to connect the finger joints with the driving unit on the arm (the total weight is less than 180 g), reducing the load on the palm. This mechanism reproduces the physiological motion range of 0−85°. Under the condition of excessive resistance, the end displacement deviation is less than 1.2 mm. Compared with the traditional rigid mechanism, the weight is reduced by 35%, significantly improving the wearing comfort and the compliance of rehabilitation training [7].

A Assist-as-Needed (AAN) control strategy for a soft finger rehabilitation robot based on an interactive torque observer, developed by the Department of Mechanical Engineering at AmirKabir University of Technology. The trajectory tracking error of this system is as low as RMSE 1.31° - 2.34°, with a smooth control response. Compared with traditional model-free methods, the error is reduced by more than 50%, and personalized assistance can be achieved without patient modeling [8].

In the journal Applied Sciences, Volume 11, 2021, there is an article titled "Design of a Wearable Finger Exoskeleton for Rehabilitation". The research proposes a new type of single-degree-of-freedom wearable finger exoskeleton that realizes the flexion and extension movements of the finger based on a linkage mechanism. The prototype is made of ABS material through 3D printing, featuring lightweight and a compact structure. Dynamic simulation shows that the maximum required torque of the metacarpophalangeal (MCP) joint is 0.0170 N·m. Structural static analysis indicates that under a driving load of 40 N, the maximum deformation is only 1.41×10−5 m, which proves that the structural stiffness meets the usage requirements. The results of the position analysis show that the range of motion of the MCP joint reaches 25.05°, which is close to the natural range of motion of the human body (26°). The experiment verified the feasibility of this design in terms of motion range, mechanical properties, and structural stability. It is suitable for post-stroke hand rehabilitation training and has the application potential of low cost and high portability [9].

To meet the grasping needs of patients with upper-limb finger motor dysfunction caused by brain-related diseases in daily life, this paper designs an under-actuated finger rehabilitation exoskeleton based on the principles of bionic kinematics and the characteristics of the four-bar linkage mechanism. The research combines the kinematic model of human finger movement for bionic design, uses resistance simulation to mimic daily grasping scenarios, and verifies the mechanical performance of the exoskeleton in assisting extension/grasping actions.

2. Design of an Underactuated Finger Exoskeleton

2.1. Design Idea

The design of this finger rehabilitation exoskeleton aims to help patients regain a certain degree of grasping ability and is comfortable enough to wear. In order to improve the ability of the finger exoskeleton to precisely control grasping, the finger rehabilitation exoskeleton is designed with a multi-link structure.During the movement of the fingers, there is a coupling relationship between the distal phalanx and the middle phalanx, and they do not move independently. Among them, in order to achieve the goals of a simple exoskeleton structure, easy control, and under-actuation, the main body of the exoskeleton uses a four-bar linkage mechanism. This mechanism can precisely control the rotation and translation of the fingertip to achieve two degrees of freedom movement.

2.2. Kinematic Analysis of Four-Bar Linkage Mechanism

As shown in Fig. 1, point A is selected as the origin of the coordinate system for the four-bar linkage mechanism, establish a coordinate system is established with the connecting rod AD as the x-axis. Define the position parameters of each rod. Define rods AD, AB, BC, and CD as L_1, L_2, L_3, and L_4 respectively. Define the angles between the rods and the x-axis as θ_1, θ_2 and θ_3 respectively, and define the angles between rod AD and BD, and between rod BD and CD as φ_1 and φ_2.

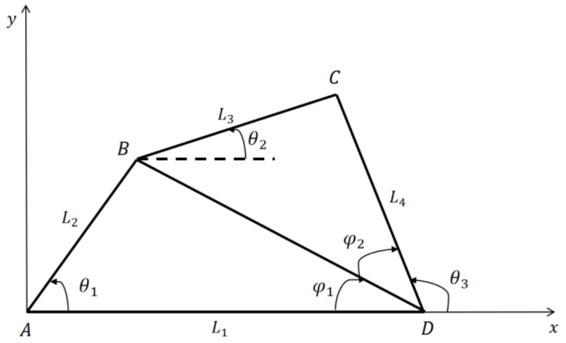

Fig. 1. Hinged four-bar linkage mechanism (Photo/Picture credit: Original).

According to the vector closure principle, in a four-bar linkage mechanism, the rods are connected end to end to form a closed quadrilateral. The position equations are established by representing each rod as a vector in the coordinate system. Starting from the origin, the sum of the vectors along the rods in the direction of another connection point should be equal to the vector from the last connection point back to the origin. According to the above position parameters, for the projections of the members DA, AB, BC, and CD in the x-axis direction (as shown in Fig. 1):

$$L_2 \cos\theta_1 + L_3 \cos\theta_2 = L_4 \cos\theta_3 + L_1 \tag{1}$$

The projections of the rods AB, BC, and CD in the y - direction (as shown in Fig. 1):

$$L_2 \sin\theta_1 + L_3 \cos\theta_2 = L_4 \sin\theta_3 \tag{2}$$

For the angle θ1, according to the cosine theorem $\cos\theta_1 = \frac{{L_1}^2+{L_2}^2-{L_{BD}}^2}{2L_1L_2}$ (as shown in Fig. 1), it can obtain:

$${L_{BD}}^2 = {L_1}^2 + {L_2}^2 - 2L_1L_2\cos\theta_1 \tag{3}$$

In triangle ABD, for angle φ_1, angle θ_1 and side L_2, side L_{BD} (as shown in Fig. 1), according to the sine theorem $\frac{L_{BD}}{\sin\varphi_1} = \frac{L_2}{\sin\theta_1}$, it has:

$$\varphi_1 = arcsin(\frac{L_2}{L_{BD}}\sin\theta_1) \tag{4}$$

For the angle φ_2, according to the cosine theorem $\cos\varphi_2 = \frac{{L_{BD}}^2+{L_4}^2-{L_3}^2}{2L_{BD}L_4}$ (as shown in Fig. 1), it can obtain:

$$\varphi_2 = arccos\frac{{L_{BD}}^2+{L_4}^2-{L_3}^2}{2L_{BD}L_4} \tag{5}$$

The angles θ_3, φ_1 and φ_2 are supplementary (as shown in Fig. 1):

$$\theta_3 = \pi - \varphi_1 - \varphi_2 \tag{6}$$

From formula (2), it gets:

$$\theta_2 = arcsin(L_4\sin\theta_3 - L_2\sin\theta_1) \tag{7}$$

By differentiating the position equations with respect to time, the velocity equations can be obtained.

Assume that the rotational speed of the driving link L_{AB} is ω_1, the rotational speed of the rod BC is ω_2, and the rotational speed of the rod CD is ω_3. Then, by differentiating time in the position equations (1) and (2) with $\theta_i = \omega_i t$, it can get:

$$L_2\omega_1\cos\theta_1 + L_3\omega_2\cos\theta_2 = L_4\omega_3\cos\theta_3 \tag{8}$$

$$L_2\omega_1\sin\theta_1 + L_3\omega_2\sin\theta_2 = L_4\omega_3\sin\theta_3 \tag{9}$$

Differentiate the velocity equations (8) and (9) with respect to time using $\omega_i = \beta_i t$, and the acceleration equations can be obtained. Here, β_2 and β_3 are the angular accelerations of the rod BC and the rod CD, respectively.

$$\begin{bmatrix} -L_3 \sin\theta_2 & L_4 \sin\theta_3 \\ L_3 \cos\theta_2 & -L_4 \cos\theta_3 \end{bmatrix} \begin{bmatrix} \beta_2 \\ \beta_3 \end{bmatrix} + \begin{bmatrix} -L_3\omega_2 \cos\theta_2 & L_4\omega_3 \cos\theta_3 \\ L_3\omega_2 \sin\theta_2 & L_4\omega_3 \sin\theta_3 \end{bmatrix} \begin{bmatrix} \omega_2 \\ \omega_3 \end{bmatrix} = \omega_1 \begin{bmatrix} L_2\omega_1 \cos\theta_1 \\ L_2\omega_1 \sin\theta_1 \end{bmatrix} \quad (10)$$

Code the rod lengths of 0.60 m, 0.240 m, 0.500 m, and 0.600 m, respectively for kinematic analysis.

(a)Line graph of angular displacement, the abscissa “Crank angleθ_1/rad” represents the crank angle, and the ordinate “Angular displacement/rad” represents the angular displacement. The blue line shows the change in the angular displacement with the crank angle. The angular displacement exhibits periodic fluctuations in the range of 0 to 200 radians, with the maximum value approaching 2 radians and the minimum value approaching -1 radians.

(b)Line graph of angular velocity, the abscissa Crank angle $\theta_1/cicr$ represents the crank angle, and the ordinate: Angular velocity/$rad{\cdot}s^{-1}$ represents the angular velocity. The blue line shows the variation of the angular velocity with the crank angle. The angular velocity fluctuates within the range of 0 to 200 revolutions. The maximum value is close to $1{\cdot}10^{12}$rad·s^{-1}, and the minimum value is close to -2×10^{12}rad·s^{-1}.

(c)Line graph of angular acceleration, the abscissa Crank angleθ_1/rad represents the crank angle, and the ordinate Angular acceleration/rad·s^{-2} represents the angular acceleration. The blue line shows the variation of the angular acceleration with the crank angle. The angular acceleration fluctuates in the range of 0 to 200 radians, with the maximum value approaching 2×10^{39}rad·s^{-2} and the minimum value approaching 0 rad·s^{-2}.

(d) Schematic diagram of the positional relationship among rods 1, 2, 3, and 4 in the four-bar linkage mechanism.

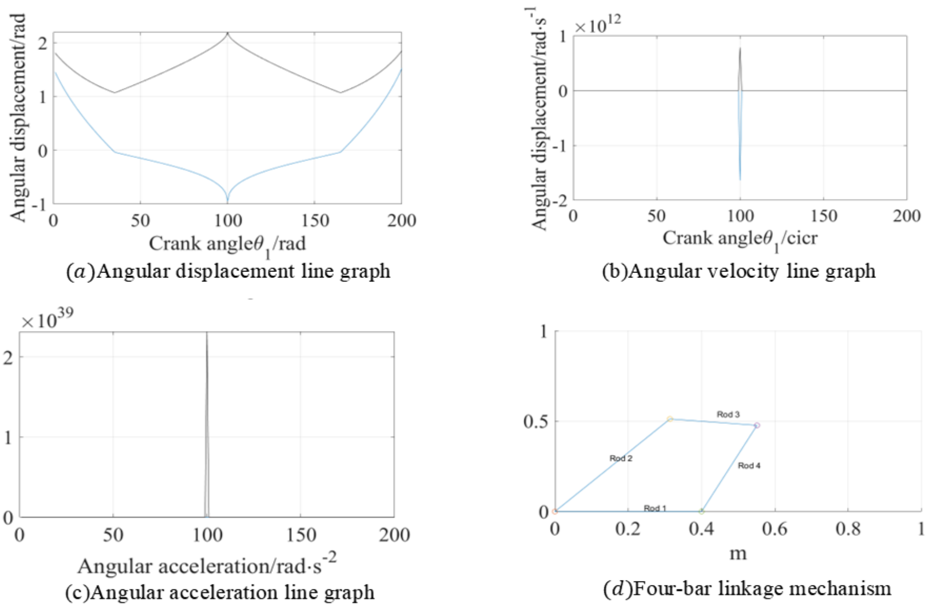

Fig. 2. Line graphs of angular displacement(a), angular velocity(b), and angular acceleration(c); Four-bar linkage mechanism(d) (Photo/Picture credit: Original).

The distal ends of the fingers are uneven. Generally, the middle finger protrudes the most, and the thumb is the shortest. The index finger may be shorter or longer than the ring finger. Except for the thumb, the little finger is the shortest among the other four fingers, but there is also great variation in the relative length of its distal end [10]. Moreover, when the fingers are in motion, there is a coupling effect between the phalanges. Therefore, to ensure the bionic effect and good grasping robustness of the finger rehabilitation exoskeleton, after referring to the average length of the index finger phalanges of Chinese adults, in this exoskeleton system, the distal phalanx is 20 mm, the middle phalanx is 25 mm, and the proximal phalanx is 40 mm. A three - stage hinged four - bar mechanism series topology is adopted to ensure the authenticity of the research.

Fix the patient's palm and the exoskeleton base plate with straps. When the finger joints bend, there is a geometric deviation between the rigid exoskeleton and the finger joints. For example, when the metacarpophalangeal joint is flexed to 60°, the offset Δd between the hinge axis of the proximal drive stage and the anatomical joint axis is 1.8 mm, which leads to relative sliding at the contact surface between the exoskeleton and the finger. Therefore, the distal phalanx is connected to the end-effector stage of the exoskeleton through a sliding groove to address this issue.

3. Simulation Analysis of Finger Exoskeleton

3.1. Material Selection

In the material selection of finger rehabilitation exoskeletons, the current mainstream exoskeleton materials in the market include aviation aluminum alloy 7075-T6, medical titanium alloy TC4, and carbon fiber T700. To pursue the characteristics of lightweight, high strength, and suitability for daily wear of the finger rehabilitation exoskeleton, both the overall finger rehabilitation exoskeleton and the platform carrying the small balls are made of 7-series aluminum alloy 7075-T6 (SN) as the material. The tensile strength of this material reaches 570 MPa, and its density is only 2.8 g/cm³. Its specific strength surpasses that of titanium alloy, significantly reducing the load on the exoskeleton, and it has an ultra-high specific strength.

Its fatigue limit reaches 159 MPa, far superior to engineering plastics, ensuring the reliability of joint components during long-term rehabilitation training, and it has excellent dynamic fatigue performance. Moreover, its price is only 1/5-1/3 of that of titanium alloy, and the material utilization rate is as high as 85%, reducing the mass-production cost and having the characteristic of a high cost-effectiveness ratio.

3.2. Simulation Environment Setup

In the simulation environment where the finger exoskeleton grabs small balls, to make it closer to real life, the gravitational acceleration vector in the simulation environment is set as $\vec{g}$=(0,0,-9.81)m/s^2 (in the Fig.2, since the finger exoskeleton is used for side - way grasping, the gravitational force is set along the y-axis). The joints are driven by motor control, and the motor speed is 4 mm/s to simulate the action of grasping objects in daily life.

3.3. Ball Grasping Simulation

In the simulation of grasping a small ball, the contact force between the finger pad and the small ball and the stability of the object during grasping are extremely important. Regarding these two factors, while keeping other parameters unchanged, the material of the small ball was changed. The small balls were made of common materials in daily life, namely plastic (PP copolymer), wood (oak), and steel (cast stainless steel) for the simulation. The contact force Fc between the finger pad and the small ball, and the displacement Δx of the small ball were collected to evaluate the grasping robustness (Fig. 3).

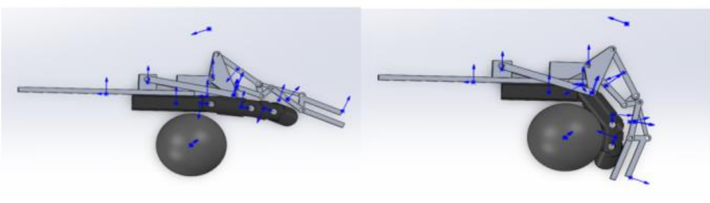

Fig. 3 Simulation of grasping small balls by a finger rehabilitation exoskeleton (Photo/Picture credit: Original).

3.4. Analysis of Experimental Results

Table 1. Data on the position of the center of mass over time

Material	Position Trend (0-0.1s)	Key Feature
Rubber	426.5mm →429mm (0.06s) → 416mm	Sharp rise & rapid drop
Oak Wood	426.5mm →429mm (0.055s) → 416mm	Gradual rise, delayed fall
Stainless Steel	428mm →470mm (0.1s)	Steady linear increase

Table 2. Data of reaction force over time

Material Type	Initial Response Time (s)	Peak Reaction Force (N)	Dynamic Fluctuation Amplitude (ΔN)	Energy Dissipation Rate* (J/s)
Rubber	0.05	-12	1.8	82%
Oak Wood	0.05	~+14 (estimated)	0.5	35%
Stainless Steel	0.055	+14	0.3	18%

According to the experimental data, stainless steel exhibits the most stable dynamic characteristics. Its center of mass shows a rigid-dominated linear rise (displacement Δ42mm as shown in Table 1), and the fluctuation of the reaction force is extremely small (Δ0.3N as shown in Table 2). Rubber, on the other hand, shows a significant viscoelastic hysteresis effect. After a brief upward rush, the center of mass drops rapidly (displacement Δ13mm as shown in Table 1), corresponding to the negative peak reaction force (- 12N as shown in Table 1) and an energy dissipation rate of 82% (as shown in Table 2). Although oak has a positive-like peak force with an ambiguous direction (about +14N as shown in Table 2) and a phenomenon of delayed stabilization of the center of mass, it shows a gradual decline (displacement Δ13mm as shown in Table 1) and moderate energy loss (35% as shown in Table 2). The experimental data indicate that this finger rehabilitation exoskeleton has good grasping robustness and manufacturing feasibility in daily life.

4. Conclusion

Based on the principle of bionic kinematics, combined with the morphological characteristics and movement mechanism of human fingers, this study designed an under-actuated finger rehabilitation exoskeleton. The design adopts a three-stage hinge four-bar mechanism in a series topology, which effectively simulates the coupling relationship between the middle phalanx and the distal phalanx of the finger, solves the tendon interference problem of traditional exoskeletons, improves the accuracy and coordination of the exoskeleton, and reduces the number of driving units. A single motor is used to achieve a multi-joint linkage, which is convenient for daily wear and suitable for daily life. Moreover, the design has a simple structure and good feasibility in physical manufacturing. It has the potential to assist patients with upper-limb motor function disorders, such as those after a stroke, in active or passive rehabilitation training, which is expected to improve the rehabilitation efficiency and reduce medical costs.

Although the kinematic and chemical simulation verifies the theoretical feasibility of the mechanism design, its construction is still under ideal conditions. The next step of work will focus on prototype fabrication and human experiment verification. The human-machine interaction interface and adaptive control strategy will be further optimized. Moreover, the integration of surface electromyography signals (sEMG) will be explored to achieve intention recognition, so as to improve the intelligent and personalized rehabilitation level of the exoskeleton.

References

[1] Du Plessis T, Djouani K, Oosthuizen C. A review of active hand exoskeletons for rehabilitation and assistance. Robotics, 2021, 10(1).

[2] Zhang F H, Lin L G, Yang L, et al. Design of an active and passive control system of hand exoskeleton for rehabilitation. Applied Sciences-Basel, 2019, 9(11).

[3] Wang C M, Yang Z H, Wang T, et al. Design and Research of a Connecting Rod and Chute Type Hand Rehabilitation Exoskeleton. Group Technology & Production Modernization, 2022, 39(01): 8-13+37.

[4] Liao B, Huang Y H, Zou X, et al. Design of finger exoskeleton based on linkage mechanism. Science Technology and Engineering, 2022, 22(17): 6958-6965.

[5] Refour E M, Sebastian B, Chauhan R J, et al. A general purpose robotic hand exoskeleton with series elastic actuation. Journal of Mechanisms and Robotics, 2019, 11 (6): 1-25.

[6] Chang Y, Meng Q Y, Yu H L. Research Progress in Hand Rehabilitation Robot Technology. Beijing Biomedical Engineering, 2018(6): 650-656.

[7] Yao H Y. Structural design and research of finger rehabilitation robot. North China University of Science and Technology, 2023.

[8] Besharati A, Taghvaeipour A, Kamali E A, et al. Assist-as-needed control of a soft rehabilitation robot for the finger using an interaction torque observer. European Journal of Control, 2025: 101395.

[9] Hernández-Santos, C., Davizón, Y.A., Said, A.R. et al. Development of a Wearable Finger Exoskeleton for Rehabilitation. Appl. Sci. 2021, 11, 4145.

[10] He G C, Zhong S Z, Liu Z J. Observation on the finger types of Chinese people: Discussion on finger types from the relative length of the distal phalanx of the finger. Acta Anatomica Sinica, 1966, (01): 50-56.